EBOLA VIRUS

A screen of approved drugs and molecular probes identifies therapeutics with anti–Ebola virus activity

Lisa M. Johansen,[1] Lisa Evans DeWald,[2] Charles J. Shoemaker,[3] Benjamin G. Hoffstrom,[1] Calli M. Lear-Rooney,[2] Andrea Stossel,[2] Elizabeth Nelson,[3] Sue E. Delos,[3] James A. Simmons,[3] Jill M. Grenier,[1] Laura T. Pierce,[1] Hassan Pajouhesh,[1] Joseph Lehár,[1,4] Lisa E. Hensley,[2] Pamela J. Glass,[2] Judith M. White,[3] Gene G. Olinger[2*†]

Currently, no approved therapeutics exist to treat or prevent infections induced by Ebola viruses, and recent events have demonstrated an urgent need for rapid discovery of new treatments. Repurposing approved drugs for emerging infections remains a critical resource for potential antiviral therapies. We tested ~2600 approved drugs and molecular probes in an in vitro infection assay using the type species, *Zaire ebolavirus*. Selective antiviral activity was found for 80 U.S. Food and Drug Administration–approved drugs spanning multiple mechanistic classes, including selective estrogen receptor modulators, antihistamines, calcium channel blockers, and antidepressants. Results using an in vivo murine Ebola virus infection model confirmed the protective ability of several drugs, such as bepridil and sertraline. Viral entry assays indicated that most of these antiviral drugs block a late stage of viral entry. By nature of their approved status, these drugs have the potential to be rapidly advanced to clinical settings and used as therapeutic countermeasures for Ebola virus infections.

INTRODUCTION

Filoviruses (*Ebolavirus* and *Marburgvirus*) are responsible for acute viral hemorrhagic fevers and are grave viral threats that continue to infect humans as well as nonhuman primates (*1*, *2*). The genus *Ebolavirus* includes five species that induce disease with case fatality rates up to 90% (*3*), whereas the single genus *Marburgvirus* has multiple virus members associated with disease with variable fatality rates (20 to 90%). Filovirus illness is characterized by fever, myalgia, headache, and gastrointestinal symptoms, and patients may also develop a maculopapular rash (*4*). Fatal outcomes correlate with increased viremia, convulsions, and disseminated intravascular coagulation with patients succumbing to a septic shock–like syndrome (*4*).

The current Ebola virus disease epidemic in Western Africa, the largest outbreak on record (*5*), underscores the urgent need for therapeutic as well as prophylactic interventions that can be easily distributed to patients, healthcare workers, and the general population. Further, this epidemic highlights the ease at which filoviruses may be accidentally imported to other countries from endemic regions by asymptomatically infected humans before onset or diagnosis of the disease. Unfortunately, to date, no approved therapeutics (small molecule or biologic agents) are available for prophylaxis or treatment of filovirus diseases. Treatment for the current Ebola virus disease outbreak relies on supportive care and judicious use of limited quantities of experimental therapeutics (*6*).

Through systematic screening of approved drugs, can discover therapeutics that can quickly be deployed for new indications (*7*–*9*). This approach identifies drugs acting via expected target mechanisms (*10*), as well as drugs acting through mechanisms that would not have been predicted (*11*). Moreover, with approved drugs, one can take advantage of known pharmacology and toxicity profiles, established safety in humans, and proven manufacturing and formulation feasibility. Therapeutics identified from such screens could be swiftly advanced to human trials and may have "off-the-shelf" availability in the event of an outbreak, such as the current Ebola virus disease epidemic.

To address the urgent need for therapeutics for prophylaxis and treatment of Ebola virus disease, we conducted a screen of approved drugs and biologically active molecular probes using an Ebola virus engineered to express enhanced green fluorescent protein (eGFP-EBOV) (*12*). We identified 171 active compounds, including 80 U.S. Food and Drug Administration (FDA)–approved drugs with significant anti-EBOV activity. A set of approved drugs was prioritized, and the antiviral activity was further validated in secondary assays, including an in vitro virus-like particle (VLP) entry assay and a murine model of EBOV disease. We identified sertraline (Zoloft), a selective serotonin reuptake inhibitor, and bepridil (Vascor), a calcium channel blocker, as having both strong in vitro and in vivo antiviral activity. Both drugs inhibited EBOV entry late in the entry pathway likely by affecting viral fusion. These drugs offer potential for repurposing for Ebola virus disease, either as single agents or in combinations, and could be used in circumstances similar to the current epidemic.

RESULTS

A screen of approved drugs identified compounds with anti-EBOV activity

A library of about 2600 biologically active small molecules composed of FDA-approved drugs and common mechanistic probes with known molecular targets was assembled to identify novel inhibitors of EBOV infection using the eGFP-EBOV (*12*). The library composition included 64% approved drugs (U.S. and ex-U.S.) and 26% probes, with the remainder of the library composed of metals, herbals, amino

[1]Horizon Discovery Inc., 245 First Street, Cambridge, MA 02142, USA. [2]U.S. Army Medical Research Institute of Infectious Diseases, 1425 Porter Street, Frederick, MD 21702, USA. [3]University of Virginia, 1340 Jefferson Park Avenue, Charlottesville, VA 22908, USA. [4]Bioinformatics Program, Boston University, 20 Cummington Street, Boston, MA 02215, USA.
*Present address: Integrated Research Facility, Division of Clinical Research, National Institute of Allergy and Infectious Diseases, B-8200 Research Plaza, Fort Detrick, Frederick, MD 21702, USA.
†Corresponding author. E-mail: gene.olinger@nih.gov

acids, drug analogs, drug metabolites, diagnostic agents, and food additives (table S1) (*7*, *13*). For the preliminary screen, compounds were screened at three-dose points. Compounds were considered active if they inhibited the eGFP signal by ≥40% and showed no or minimal effects on cell viability through the parallel antiproliferation screen in uninfected host Vero E6 cells (table S1). From this preliminary screen, a set of about 171 active compounds was identified (table S2), of which 80 compounds are FDA-approved drugs. A total of 98 active compounds are approved in either the U.S. or ex-U.S. A scatter plot displays an overview of the antiviral activity versus cell viability for each compound screened and identification of active compounds (fig. S1).

The composition of the screened chemical library covers about 50 distinct cellular mechanisms that encompass many molecular targets (Fig. 1 and table S1). The active compounds identified from the screen spanned multiple cellular mechanisms, including compounds that affect cell signaling, protein processing, and ion transport (Fig. 1). Additionally, we identified a large number of previously reported selective estrogen receptor modulators (SERMs) (*11*) and compounds that inhibit the histamine H1 receptor (Fig. 1).

A set of 30 compounds was prioritized for confirmation of antiviral activity in both the Vero E6 and human HepG2 cell lines in an eight-point dose-response curve (Table 1 and Figs. 2 and 3). The prioritization was based on the antiviral activity and selectivity, approval in the U.S. or ex-U.S., and systemic delivery route of administration and exposure. For class effect hits, such as the SERMs or antihistamines, class representatives were selected. Mechanistic probes were not prioritized. Representative active drugs include aripiprazole (an antipsychotic drug), piperacetazine (another antipsychotic drug currently used as a veterinary sedative), benztropine (an anticholinergic used to treat Parkinson's disease), clemastine (an antihistamine), bepridil and lomerizine (calcium channel blockers), and clomipramine and sertraline (antidepressant drugs). The eight-point dose-response data for the remaining 30 prioritized active compounds are shown in figs. S2 to S5.

Prioritized active compounds inhibit EBOV viral entry in vitro

We previously reported that class II cationic amphiphilic drugs (CADs) can act as EBOV entry inhibitors (*11*, *14*). CADs contain a hydrophobic tertiary amine with clearly segregated hydrophobic and hydrophilic segments. An analysis of the structures of the 30 prioritized active compounds revealed that 17 of the 30 prioritized compounds are CADs (Table 2), including clomiphene and toremifene, which were previously reported as active compounds (*11*, *14*). Additionally, 8 of the 30 active compounds are amphiphiles with similar hydrophobic and hydrophilic organization. The approved pharmacologic mechanisms of therapeutic action vary considerably between these drugs, despite their similar CAD structural properties.

Given the relatively large number of CADs in our set of 30 active compounds, we evaluated this set of drugs for their ability to inhibit EBOV entry using VLPs expressing EBOV glycoprotein ($GP_{1,2}$) and containing a β-lactamase (BlaM) entry reporter (*14*–*16*). Each compound was initially tested at one concentration targeted between the IC_{50} and IC_{90} concentrations obtained from the eight-point dose-response confirmation with eGFP-EBOV. Results of these VLP entry assays indicate that 25 of the 30 active compounds tested inhibited EBOV-VLP entry by >90% (Table 2). The autofluorescence of quinacrine, an antimalarial drug also classified as a CAD, obscured the assay results, and we could not evaluate its ability to inhibit EBOV-VLP entry. All other CADs examined were found to be EBOV entry inhibitors, supporting our previous observations. We observed that the remaining 4 non-CADs of 30 active

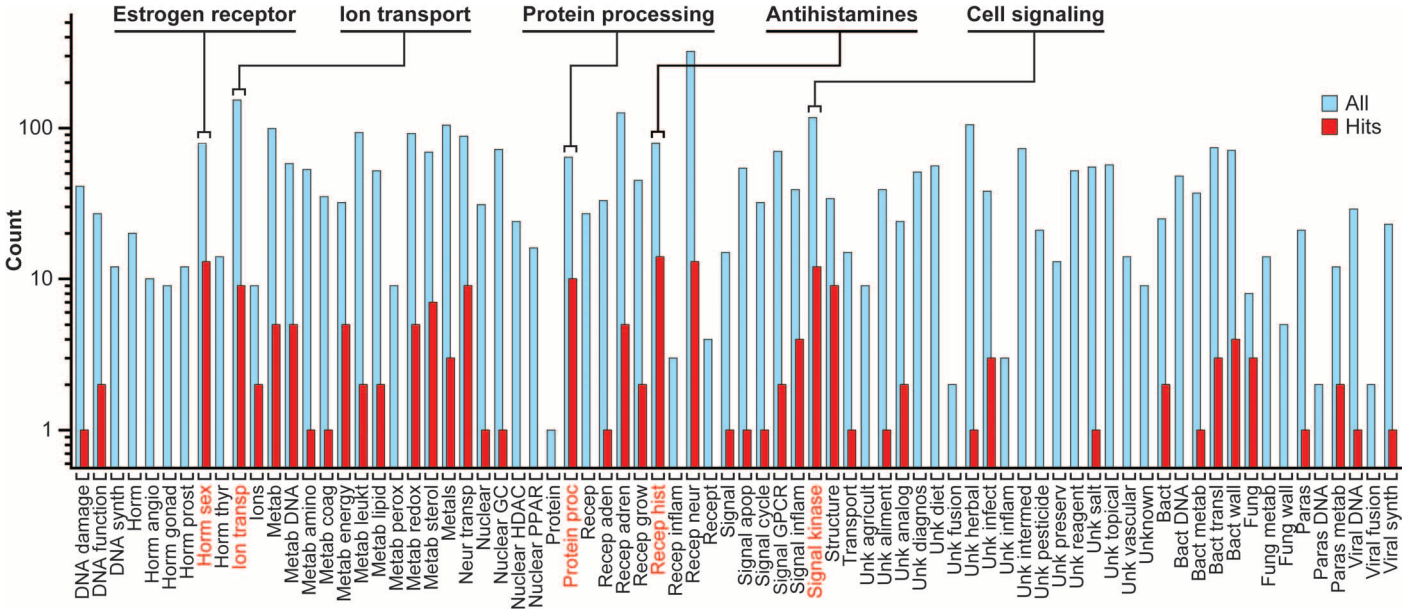

Fig. 1. Mechanistic overview of compound library. Histogram showing the cellular compound mechanisms from the drug library across the horizontal axis. The vertical axis indicates the number of compounds with that particular mechanism in log scale. Blue bars indicate the number of all compounds that contain a particular mechanism (All). Red bars indicate the number of active compounds identified (Hits) per each mechanism. The screen identifies a number of compounds that are SERMs and antihistamines, and compounds that affect ion transport and protein processing or cell signaling pathways. GC, glucocorticoid nuclear receptor; HDAC, histone deacetylase; PPAR, peroxisome proliferator–activated receptor; GPCR, G protein (heterotrimeric guanine nucleotide–binding protein)–coupled receptor.

Table 1. Anti-EBOV activity and cytotoxicity of active compounds. Parentheses indicate the SE for IC_{50} calculations. Table summarizes data shown in Fig. 2 and 3 and figs. S3 to S6. %I, maximum percent inhibition based on the curve fit; IC_{50}, drug concentration in μM at which 50% inhibition of viral infection or host viability (without virus) was observed.

Drug name	Vero E6				HepG2			
	IC_{50} eGFP-EBOV μM (SE)	%I eGFP-EBOV	IC_{50} Host μM (SE)	%I Host	IC_{50} eGFP-EBOV μM (SE)	%I eGFP-EBOV	IC_{50} Host μM (SE)	%I Host
Aripiprazole	8.1 (0.42)	86.7	–	20.7	3.76 (0.18)	94.7	19.4 (1.61)	82
Astemizole	6.17 (1.34)	96.5	–	37.9	1.37 (0.038)	91.4	11.1 (0.055)	99.6
Atovaquone	0.437 (0.016)	73.9	–	35.4	–	5.71	–	3.62
Azacitidine	8.97 (2.6)	74.7	–	27.9	10.3 (1.00)	89.9	–	33.1
Benztropine	8.07 (0)	89.1	–	21.0	2.82 (0.13)	93.9	–	18.1
Bepridil	5.08 (0.38)	97	–	21.1	3.21 (0.15)	91.2	–	49.3
Clemastine	5.44 (0.32)	95.8	–	39.8	0.652 (0.037)	93.3	–	43.7
Clomiphene*	2.42 (0.045)	96.4	–	26.2	0.755 (0.046)	92.0	15 (1.28)	92
Clomipramine	11.4 (0.15)	96.1	–	21.1	2.57 (0.16)	89.9	–	23.5
Dasatinib	16.5 (4.6)	64.2	–	35.6	4.23 (0.20)	94.1	25.8 (0.80)	71.3
Efavirenz	10.7 (2.0)	63.9	–	7.38	13.5 (2.07)	86	–	9.64
Flupentixol	5.78 (0.20)	95.9	–	41.9	1.59 (0.25)	74.5	–	16.5
Fluphenazine	5.54 (0.19)	96.8	–	46.4	3.05 (1.68)	92	–	30
Hycanthone	10.9 (0.85)	96.8	–	42.9	5.96 (0.39)	96.2	16.6 (0.82)	62.9
Lomerizine	11.4 (1.8)	89.9	–	19.7	2.42 (0.12)	91.8	–	43.9
Maprotiline	9.63 (0.01)	98.6	–	26.3	2.86 (0.15)	92.6	–	41.3
Mycophenolate mofetil		43.8	–	3.27	0.29 (0.15)	88.6	–	17.6
Paroxetine	7.45 (0.41)	96	–	39.9	1.38 (0.076)	92	23.6 (0.18)	94.8
Pimozide	3.12 (0.11)	96.8	–	20.3	1.67 (0.044)	91	18.9 (0.18)	99.4
Piperacetazine	12.3 (0.85)	96.2	–	23.1	3.3 (0.16)	95.4	–	28.8
Prochlorperazine	5.96 (0.42)	96.3	–	42.8	3.59 (0.19)	94.7	–	27.3
Quinacrine	5.71 (0.61)	92.3	23.6 (8.5)	63.4	1.03 (0.052)	86.2	12.9 (1.54)	98.6
Sertraline	3.13 (0.24)	96.2	–	29.4	1.44 (0.057)	95	18 (0.53)	54.4
Simvastatin	44.6 (0.79)	55.7	–	28.5	–	35.3	–	11.8
Strophanthin	0.0346 (0.020)	74.3	–	28.8	0.0207 (0.0014)	86.8	0.0569 (0.00047)	68.4
Teicoplanin	7.28 (0.46)	84.6	–	2.72	2.43 (0.16)	77	–	2.33
Terconazole†	8.26 (0.32)	96.6	–	33.2	2.38 (0.068)	91.8	–	36.5
Thioridazine	6.24 (0.79)	95.4	10.2 (9.06)	93.1	2.06 (0.12)	93.4	21.6 (0.78)	99.4
Toremifene*	0.162 (0.048)	93.5	–	11.4	0.026 (0.0013)	94.9	–	5.43
Vinorelbine		25.6	–	27.9	0.858 (0.034)	78.8	–	32.9

*EBOV antiviral activity also described by Johansen *et al.* (*11*). †EBOV antiviral activity also described by Shoemaker *et al.* (*14*).

compounds—atovaquone, azacitidine, mycophenolate mofetil, and strophanthin—did not inhibit VLP entry, indicating that these compounds block at a step that is post-entry in the EBOV infection cycle.

Several drugs offer protection in the murine EBOV infection model

To test if the antiviral activity observed with the active compounds in vitro translated to in vivo EBOV infection, we evaluated several entry inhibitors in a murine EBOV infection model using a mouse-adapted EBOV (ma-EBOV) strain (*17*, *18*). Intraperitoneal inoculation of ma-EBOV results in acute onset of severe illness 3 to 4 days after inoculation, with high-level viral replication observed in the liver and spleen, multifocal hepatic necrosis, and a rapid increase in viremia to titers $>10^8$ plaque-forming units (PFU)/ml (*17*, *18*).

We previously reported that treatment with the CADs clomiphene and toremifene resulted in significant survival benefit in the murine EBOV infection model (*11*). Bepridil and sertraline (both CADs), along with several other drugs (CADs, amphiphiles, and one anhydride) (Fig. 4 and table S3), were selected for evaluation in the murine infection model. In these studies, female C57BL/6 mice (5 to 8 weeks old) were challenged intraperitoneally with the target virus exposure dose of 1000 PFU of ma-EBOV. One hour after infection, the animals were treated with a drug or vehicle control for 10 days, and survival

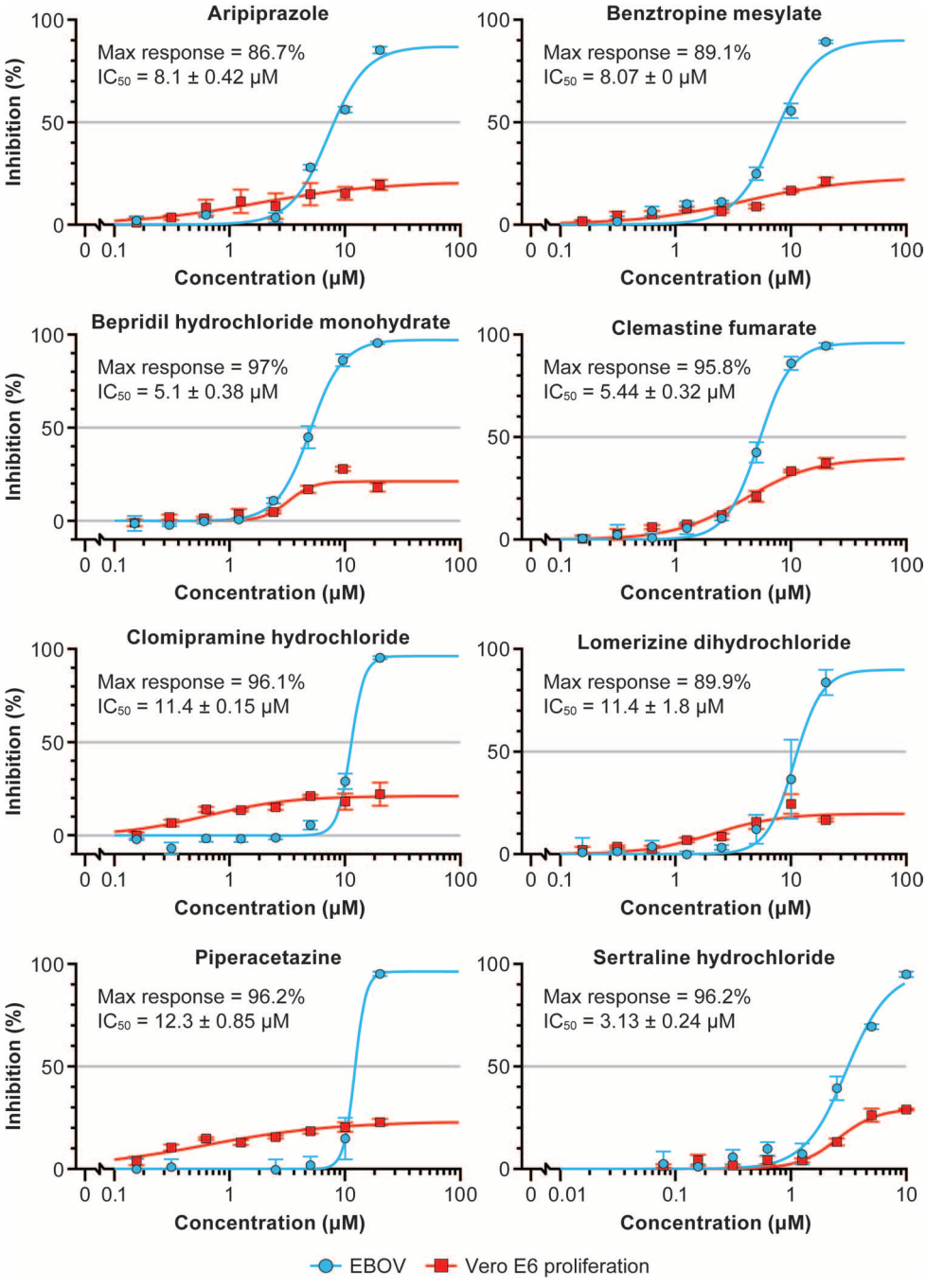

Fig. 2. Confirmatory eight-point dose-response curves for select active compounds in Vero E6 cells. Compounds were evaluated using the eGFP-EBOV screening assay. The percent inhibition of the compound in the EBOV assay is shown in blue, and the percent cytotoxicity of the compounds on the host cell is shown in red. The maximum percent inhibition observed (Max response) of EBOV and IC_{50}s are indicated. Error bars indicate the SEM. Results are from a minimum of two replicates. Data in Vero E6 cells for additional active compounds comprising a set of 30 prioritized compounds are shown in figs. S2 and S3.

was monitored for 28 days after exposure. The dose and regimens for each treatment were selected on the basis of the human equivalent dose and reported half-life for the compounds. Doses were also selected in an attempt to avoid acute toxicity yet achieve high enough plasma exposure in the mice to observe a positive effect on survival. Bepridil was administered at 12 mg/kg twice daily (BID) and sertraline was administered at 10 mg/kg BID. For both bepridil and sertraline, treatment of infected mice resulted in statistically significant survival benefits as shown in the Kaplan-Meier plots (Fig. 4). Percent survival of mice ranged from 70% (sertraline, $P = 0.0019$) to 100% (bepridil, $P < 0.0001$).

Most of the additional compounds evaluated in this model did not result in statistically significant survival benefits, and, in some cases, no survival benefit was observed except for clomipramine at the dose regimens tested (table S3). Further optimization of dose regimens for these compounds may be required to observe an effect on survival in this model.

In summary, the in vitro antiviral activity observed for four entry inhibitor drugs identified through this screen—bepridil, sertraline, clomiphene, and toremifene—translated to significant survival benefits in the murine EBOV infection model. These results support the use of entry inhibition as a target for EBOV intervention.

Bepridil and sertraline inhibit EBOV entry at a step after internalization

EBOV entry is mediated exclusively by the viral glycoprotein ($GP_{1,2}$) (*19*, *20*), and multiple steps in the process of entry could be blocked to prevent infection. These steps include binding to the host cell surface, internalizing into endosomes through macropinocytosis (*21*), trafficking through the endocytic pathway, and cleaving the GP_1 subunit by endosomal cathepsins (*15*, *22*, *23*). Later steps of viral entry include binding of cleaved (19 kD) GP to the endolysosomal membrane Niemann-Pick C1 (NPC1) protein (*24*–*26*), triggering of fusion (*15*, *27*–*29*), and finally fusing of viral and endolysosomal membranes, which releases the nucleocapsid into the cytoplasm to begin replication.

Bepridil and sertraline were selected for further investigation of the mechanism for inhibiting viral entry and exploration of antiviral activity across Ebola virus species based on approved drug status and positive activity in the murine infection model. As a first step in evaluating the antiviral mechanism for bepridil and sertraline, multiple concentrations of bepridil and sertraline were evaluated in the EBOV-VLP entry assay (Fig. 5A). Results indicate that both compounds inhibit EBOV-VLP entry in a dose-dependent manner. We next asked if either bepridil or sertraline affects entry of other

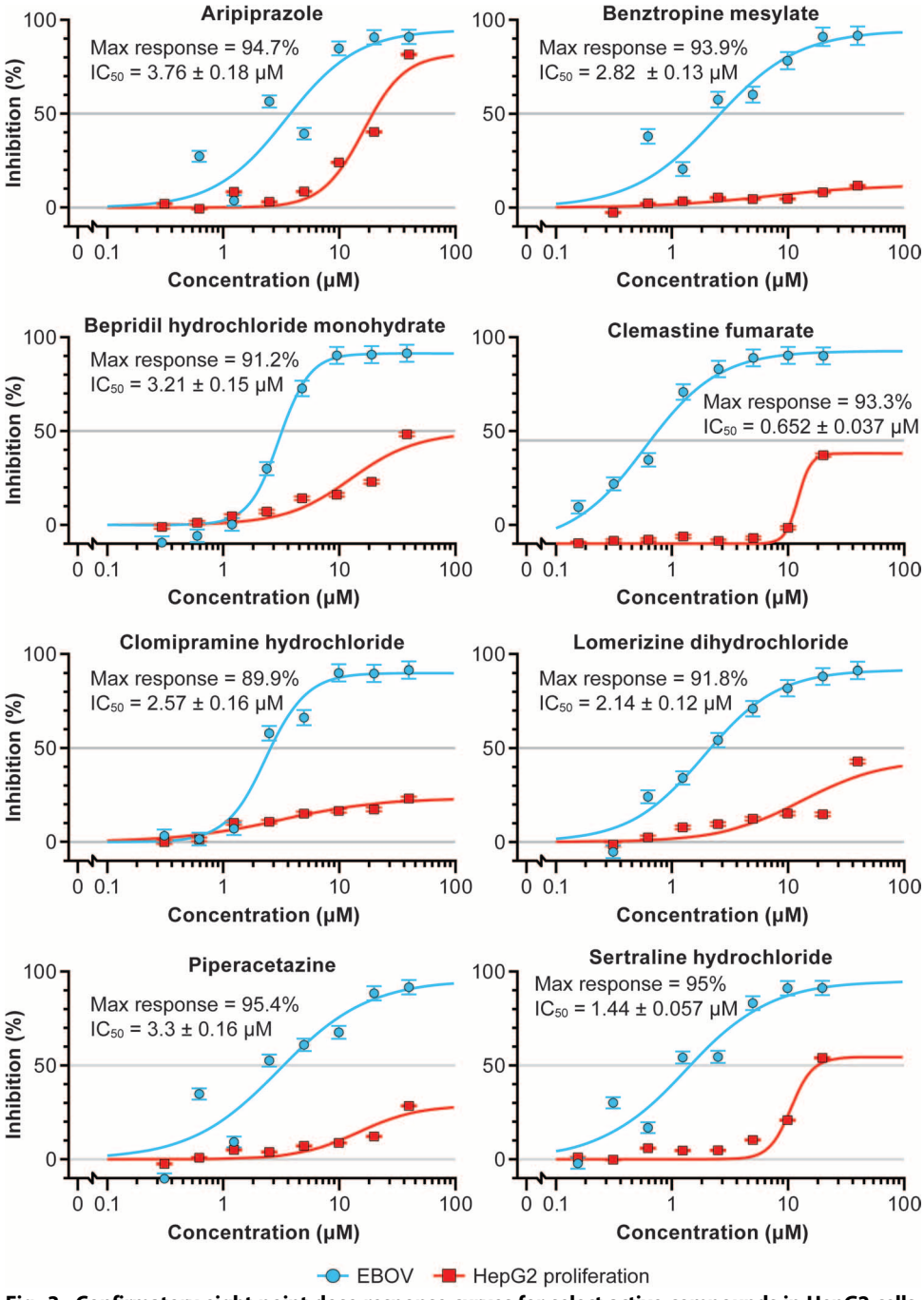

Fig. 3. Confirmatory eight-point dose-response curves for select active compounds in HepG2 cells. Compounds were evaluated using the eGFP-EBOV screening assay. The percent inhibition of compounds in the EBOV antiviral assay is shown in blue, and the cytotoxic effect of the compounds on the host cell is shown in red. The maximum percent inhibition observed (Max response) of EBOV and IC_{50}s are indicated. Error bars indicate the SEM. Results are from a minimum of two replicates. Data in HepG2 cells for additional active compounds comprising a set of 30 prioritized compounds are shown in figs. S4 and S5.

viruses that enter through endosomes. At the highest concentrations tested, no inhibition was seen for VLPs bearing the vesicular stomatitis virus (VSV)–G glycoprotein. However, inhibition was seen for VLPs bearing the glycoprotein of the arenavirus, lymphocytic choriomeningitis virus (LCMV-GP) (Fig. 5, B and C).

Bepridil and sertraline were also examined for their ability to inhibit EBOV entry through inhibition of particle internalization. To examine this ability, VLPs containing a fluorescent-tagged VP40 marker were used as described previously (*14*). For these experiments, 293AD cells were treated with bepridil, sertraline, 5-(*N*-ethyl-*N*-isopropyl)-amiloride (EIPA), or vehicle. Neither bepridil nor sertraline inhibited the amount of intracellular VLPs after 1 hour of binding (at 4°C) and 1 hour of internalization (at 37°C). However, EIPA, a known inhibitor of macropinocytosis, did inhibit the entry of VLPs into 293AD cells (Fig. 6A). This implies that neither bepridil nor sertraline inhibits either VLP binding to or internalization from the cell surface.

Bepridil and sertraline were evaluated for their effect on the activity of cathepsin B or cathepsin L, endosomal proteases that prime $GP_{1,2}$ for cellular entry (*15*, *23*). Both drugs were added independently to cells for 1 hour at 5 and 10 μM. Epoxysuccinyl-L-leucylamido-3-methylbutane ethyl ester (EST), a cysteine protease inhibitor, was used as a positive control for cathepsin inhibition (*15*). The cells were lysed and assayed for enzyme activity at a pH of 5 (*14*, *24*). Neither bepridil (5 or 10 μM) nor sertraline (at the lower concentration of 5 μM) directly inhibited the activity of either cathepsin B or cathepsin L, which cleave EBOV-GP_1 (Fig. 6B).

We also evaluated whether the drugs affected endosome acidification, which is required for cathepsin priming of GP_1 and perhaps for GP_2-mediated viral fusion for EBOV entry (*27*, *29*). Endosome acidification was assessed using LysoTracker Red, which is a probe for low pH organelles. Cells were treated with vehicle, bepridil and sertraline (at both 5 and 10 μM), or a positive control for inhibition of acidification, NH_4Cl (10 mM). Although strong inhibition of acidification was observed with NH_4Cl, inhibition was not noted with bepridil or sertraline at 5 μM (fig. S6). At 10 μM, inhibition of acidification was observed with bepridil and sertraline but not to the extent observed with NH_4Cl (fig. S6). Thus, at concentrations that strongly block entry, bepridil and sertraline appear to have minimal impact on entry steps relying on endosome acidification.

Similar with the other CADs identified from our current and previous screen, bepridil and sertraline may be affecting steps late in the entry pathway, either at VLP trafficking to the endolysosome where fusion

Table 2. VLP entry inhibition results. Conc, concentration tested in initial VLP-$GP_{1,2}$ entry inhibition assay in SNB19 cells. Yes indicates inhibition of >90%.

Drug name	Structure	Conc (μM)	Inhibit EBOV-VLP entry
Aripiprazole	Amphiphile	10	Yes
Astemizole	Amphiphile	5	Yes
Atovaquone	Phenol	0.8	No
Azacitidine	Carbohydrate	10	No
Benztropine	CAD	10	Yes
Bepridil	CAD	10	Yes
Clemastine	CAD	4	Yes
Clomiphene*	CAD	5	Yes
Clomipramine	CAD	10	Yes
Dasatinib	CAD	10	Yes
Efavirenz	Anhydride	10	Yes
Flupentixol	CAD	10	Yes
Fluphenazine	CAD	10	Yes
Hycanthone	CAD	10	Yes
Lomerizine	Amphiphile	10	Yes
Maprotiline	CAD	10	Yes
Mycophenolate mofetil	Amphiphile	1	No
Paroxetine	Amphiphile	10	Yes
Pimozide	Amphiphile	10	Yes
Piperacetazine	Amphiphile	10	Yes
Prochlorperazine	CAD	10	Yes
Quinacrine	CAD	10	Undetermined†
Sertraline	CAD	10	Yes
Simvastatin	Ester	10	Yes
Strophanthin	Carbohydrate	0.1	No
Teicoplanin	CAD	10	Yes
Terconazole‡	CAD	12	Yes
Thioridazine	CAD	10	Yes
Toremifene*	CAD	0.8	Yes
Vinorelbine	Amphiphile	5	Yes

*Entry inhibition activity also described by Johansen *et al.* (*11*). †Quinacrine is an autofluorescent compound, and its ability to inhibit EBOV-VLP entry could not be assessed in this assay. ‡Entry inhibition also described by Shoemaker *et al.* (*14*).

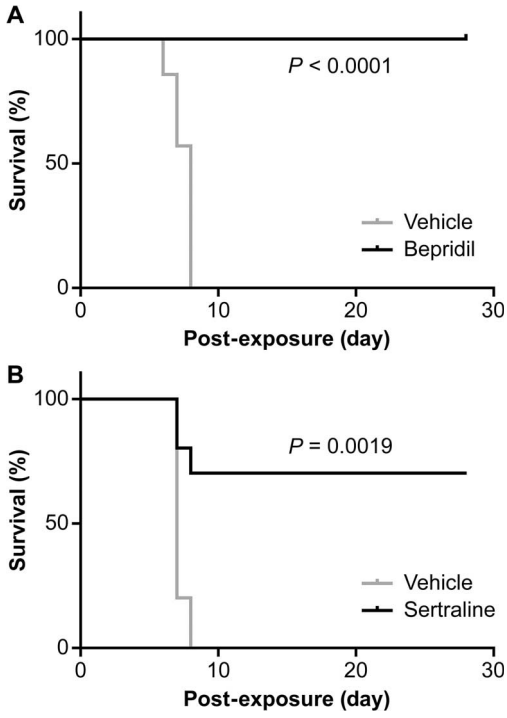

Fig. 4. Post-EBOV challenge effect of bepridil and sertraline on survival rate of mice. (**A**) Post-inoculation treatment with bepridil is 100% effective in protecting EBOV-infected animals. All mice in the vehicle control group succumbed to disease by day 9. $n = 10$ for both the vehicle and bepridil treatment groups. (**B**) Post-inoculation treatment with sertraline indicates that 70% of the EBOV-infected mice survived. Mice in the vehicle control group succumbed to disease by day 8. $n = 10$ for both the vehicle and sertraline treatment groups. The P value was determined using Fisher's exact test.

occurs or at a step in triggering of the fusion process. Therefore, both bepridil and sertraline were assessed for their ability to affect trafficking of EBOV-VLPs to $NPC1^+$ endolysosomes (Fig. 6C and fig. S7). First, fluorescently tagged EBOV-VLPs were bound to and internalized into cells. Cells were then fixed, stained for NCP1, and imaged on a confocal microscope, and images were analyzed for Manders colocalization coefficient (of VLPs with NPC1) as described in (*30*). Results indicate that although the positive control compound, nocodazole, inhibited trafficking, neither bepridil nor sertraline had any significant impact on trafficking. Cytotoxicity experiments indicated that the concentrations of bepridil and sertraline used in the entry experiments (Figs. 5 and 6) had no impact on cell viability (fig. S8).

Several CADs tested appear to block virus entry through an NPC1-dependent pathway despite no apparent direct interaction between CADs and NPC1 (*14*). In studies using VSV pseudovirions bearing EBOV-GP to infect matched Chinese hamster ovary (CHO) cells expressing basal or elevated levels of NPC1, higher concentrations of the CADs were required to inhibit pseudovirion infection in NPC1-overexpressing cells (*14*). Similar to a previous study, we compared the level of EBOV-GP pseudovirion infection in parental CHO cells to CHO cells overexpressing NPC1 (*14*) using U18666A (a CAD) as positive control. As expected, higher concentrations of U18666A were required to block EBOV infection in NPC1-overexpressing versus parental CHO cells (fig. S9). After pretreatment of both types of EBOV-GP–pseudoinfected CHO cells with sertraline or bepridil, we also observed dose shifts with both drugs, although the magnitude of the shifts appeared somewhat smaller than that observed with U18666A. This behavior is distinct from that of the cysteine protease inhibitor E64d (also known as EST), which does not exhibit a dose shift in NPC1-overexpressing cells (fig. S9) (*14*). Thus, CADs in general appear to block entry late in the pathway close to NPC1-dependent viral fusion.

Bepridil and sertraline exhibit pan anti-filovirus activity in vitro

To explore the antiviral utility across native filovirus strains, bepridil and sertraline were tested against different species of *Ebolavirus*,

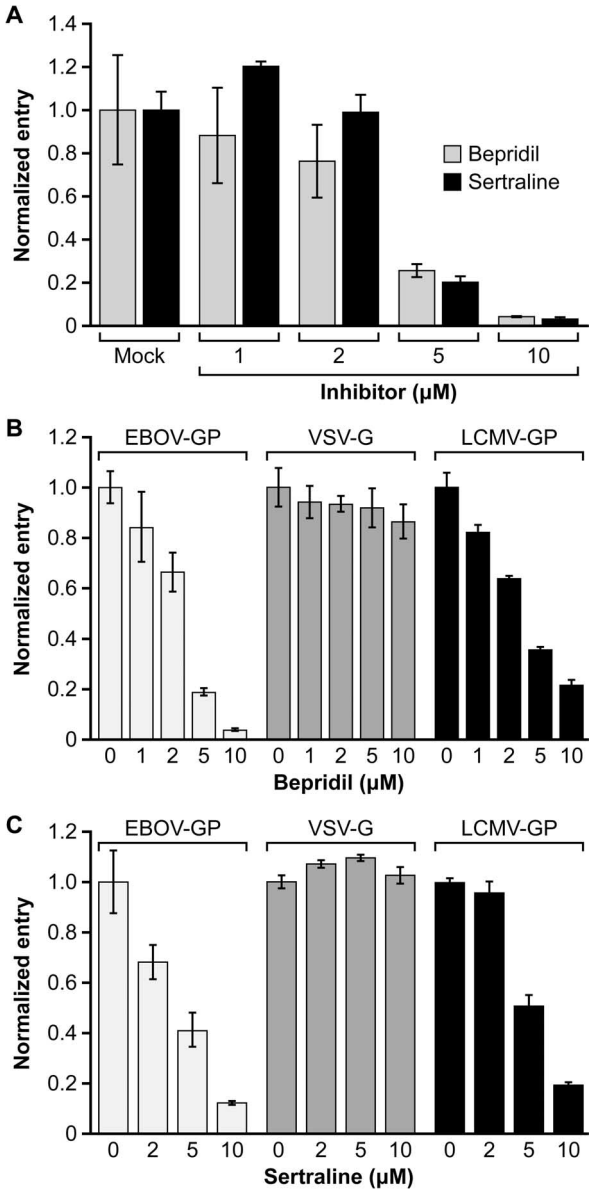

Fig. 5. Effect of bepridil and sertraline on VLP entry. Bepridil and sertraline were tested for their ability to inhibit entry of VLPs displaying EBOV-$GP_{1,2}$ glycoprotein (VLP-GP) into 293AD cells at the indicated concentrations. (**A**) Results show that both bepridil and sertraline inhibit VLP-GP entry in a dose-dependent fashion. The average normalized entry values for the two untreated (Mock) sets of samples were 19 and 24%. (**B** and **C**) Comparison of effects of bepridil (B) and sertraline (C) on entry of VLPs displaying EBOV-$GP_{1,2}$, VSV-G, or LCMV-GP. In (B), the % entry values for untreated samples (0 μM drug) were 32, 51, and 52% for EBOV-$GP_{1,2}$, VSV-G, or LCMV-GP, respectively. In (C), the % entry values for untreated samples (0 μM drug) were 10, 79, and 55% for EBOV-$GP_{1,2}$, VSV-G, or LCMV-GP, respectively. The experiment in (C) was conducted two additional times with highly similar results, even when % entry values for untreated samples were as low as 6% for entry mediated by VSV-G and 4% for entry mediated by LCMV-GP. For all panels, triplicate samples were analyzed, and error bars represent SD of the mean. Results confirm that both bepridil and sertraline inhibit entry mediated by EBOV-$GP_{1,2}$. Although these drugs have no effect on entry mediated by VSV-G, they inhibit entry mediated by LCMV-GP, albeit at somewhat higher doses than for EBOV-$GP_{1,2}$. Entry values were normalized to that observed in untreated cells.

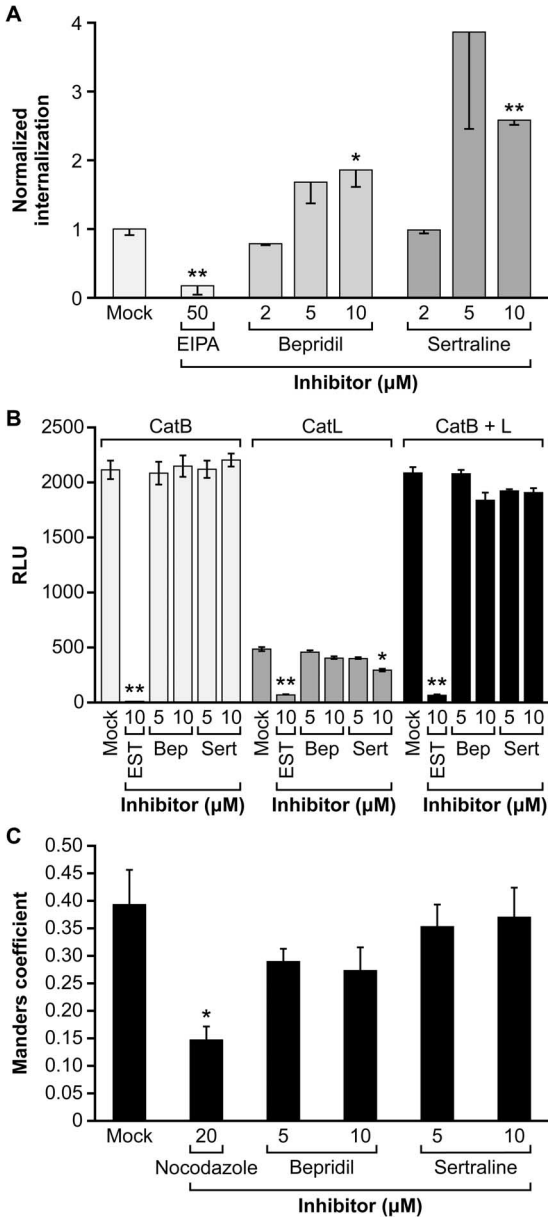

Fig. 6. Sertraline and bepridil do not inhibit EBOV-VLP–$GP_{1,2}$ internalization, cathepsin processing, or traffic to $NPC1^+$ endolysosomes. (**A**) Bepridil, sertraline, EIPA (50 μM), an inhibitor of macropinocytosis, and vehicle were tested for their ability to inhibit internalization of VLPs with the EBOV-$GP_{1,2}$ glycoprotein. Samples were analyzed in duplicate or triplicate in four experiments, and the average internalization for mock-treated samples was 30.5%. (**B**) Bepridil, sertraline, positive control EST (10 μM), a cysteine protease inhibitor, and vehicle were evaluated for effects on the activities of cathepsin B (CatB) or cathepsin L (CatL) (singly and combined; some inhibition of CatL activity was seen with 10 μM of sertraline). Samples were analyzed in triplicate. (**C**) Bepredil, sertraline, positive control nocodazole (20 μM), a microtubule disruptor, and vehicle were tested for effects on trafficking of VLP-$GP_{1,2}$ to $NPC1^+$ endolysosomes (in 293AD cells). Eighteen microscope fields were analyzed to calculate Manders colocalization coefficients. Error bars indicate SE of average values. Asterisks indicate values that are statistically different from mock-treated samples at $P < 0.02$ as determined using a Student's t test: $^{**}P < 1 \times 10^{-4}$ and $^{*}P < 0.003$ (A); $^{**}P < 3 \times 10^{-5}$ and $^{*}P < 0.002$ (B); and $^{*}P < 0.001$ (C).

namely, *Zaire ebolavirus* (EBOV/Kikwit also known as EBOV-95) and *Sudan ebolavirus* [Sudan virus (SUDV)], as well as two members of the species *Marburg marburgvirus*, Marburg virus (MARV) and Ravn virus (RAVV). Sertraline was also tested against EBOV/Mayinga strain, also known as EBOV-76. The activity of the compounds against the native strains was evaluated by cell-based enzyme-linked immunosorbent assay (ELISA). For this assay, viral isolates were used to infect Vero E6 cells in the presence of vehicle, bepridil, or sertraline (concentration range of 0.08 to 20 μM). Inhibition of viral infection was assessed at 48 hours after inoculation by fixing cells and staining with antibodies specific to the viral glycoproteins. The cell-based ELISAs demonstrated that the compounds inhibited viral infection across all of the native strains tested (Figs. 7 and 8). These results indicate that bepridil and sertraline broadly inhibit filovirus infections in vitro.

DISCUSSION

The goal of this study was to identify drugs that inhibit EBOV infection from a library of approved drugs (U.S. and ex-U.S.) and targeted molecular probes. Eighty FDA-approved drugs were identified with specific anti-EBOV activity, and a set of 30 drugs was prioritized for additional evaluation. From filamentous VLPs assays, we discovered that 25 of the 30 drugs blocked a step in viral entry. Among these 25 drugs, most drugs are CADs or amphiphiles. Four drugs tested did not inhibit viral entry, indicating that these compounds block a step that is post-entry in the EBOV infection cycle. These four drugs (all non-CADs) include atovaquone, azacitidine, mycophenolate mofetil, and strophanthin. Atovaquone acts as a dihydroorotate dehydrogenase inhibitor, an enzyme important for de novo biosynthesis of pyrimidine (*31*). Azacitidine is a pyrimidine nucleoside analog that functions as an antimetabolite of cytidine (*32*) and inhibits human inmmunodeficiency virus type 1 by inducing increased mutagenesis after incorporation (*33*). Mycophenolate mofetil is an inosine monophosphate dehydrogenase inhibitor and is known to inhibit replication of other RNA viruses through depletion of the guanosine triphosphate pool (*34*, *35*). Strophanthin is a cardiac glycoside that inhibits the replication of other RNA viruses (*36*–*38*).

A subset of compounds was also evaluated for their ability to inhibit EBOV in a murine model of infection. The results here, along with previous data (*11*), indicate that four drugs have significant survival benefits in this infection model: bepridil, sertraline, clomiphene, and toremifene. Bepridil and sertraline were further evaluated for their antiviral mechanism of action and spectrum of activity across native filovirus strains. Both drugs showed broad-spectrum antiviral activity across the native filovirus strains evaluated. Similar to clomiphene and toremifene, bepridil and sertraline appear to be inhibiting a step late in the entry process, after trafficking to $NPC1^+$ endolysosomes (*11*).

Bepridil, sertraline, and other identified CADs may block entry by targeting endolysosomal proteins whose function is somehow required for EBOV entry or by affecting the physiochemical properties of the endosomes. Several CADs identified in our screen, including bepridil and sertraline, are functional inhibitors of acid sphingomyelinase (FIASMAs) through an indirect mechanism (*39*, *40*). Acid sphingomyelinase (ASM) on the inner leaf of the endolysosomal membrane has been shown to be required for efficient Ebola virus infection (*41*), and thus, this may be one mechanism for how CADs mediate the block to viral entry. FIASMAs inhibit ASM via an indirect mechanism where the positively charged FIASMAs insert into the inner leaf of the endolysosomal membrane and dislodge the negatively charged ASM that is then degraded. Thus, CADs may affect the physiochemical properties of the lipid bilayer (*42*), which ultimately affects viral fusion.

Bepridil may also be mediating its EBOV entry block, in part, by its primary pharmacological target. Recent studies have implicated a role for calcium signaling in EBOV viral entry (*43*, *44*). Bepridil

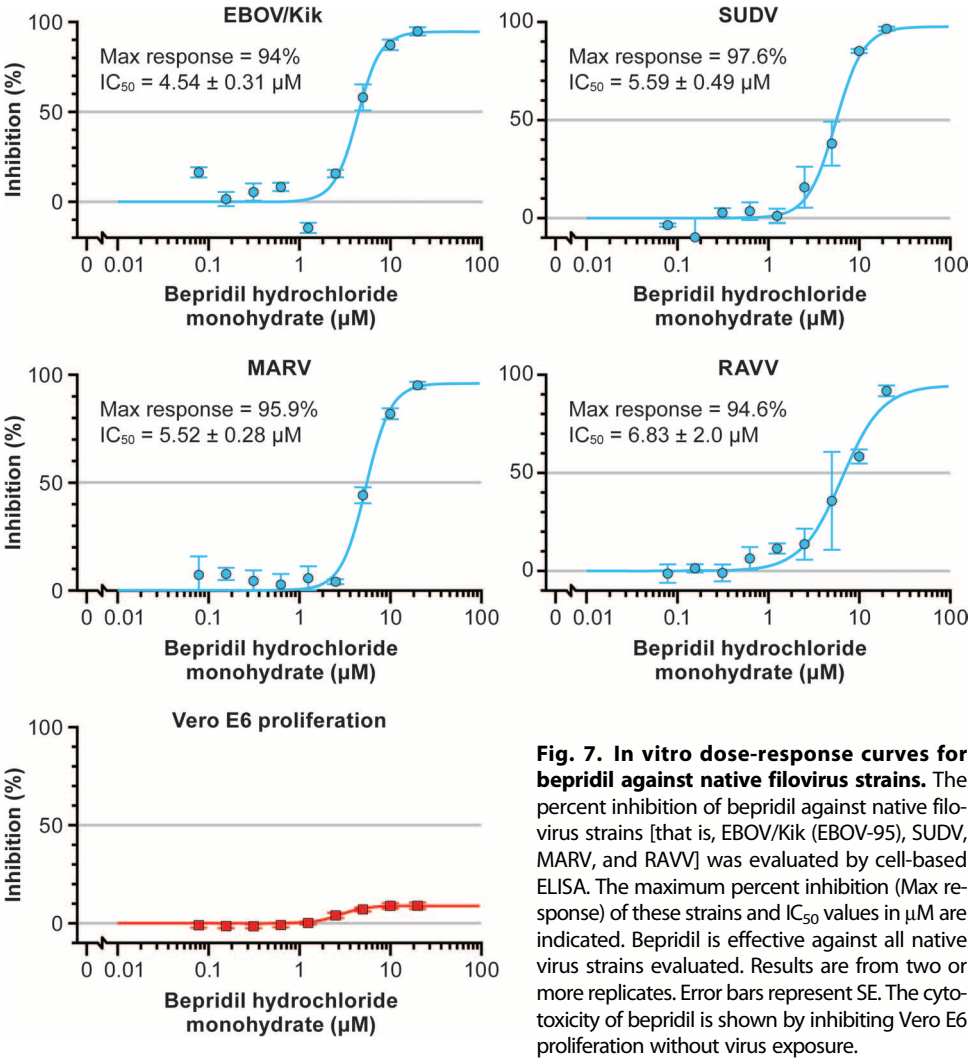

Fig. 7. In vitro dose-response curves for bepridil against native filovirus strains. The percent inhibition of bepridil against native filovirus strains [that is, EBOV/Kik (EBOV-95), SUDV, MARV, and RAVV] was evaluated by cell-based ELISA. The maximum percent inhibition (Max response) of these strains and IC_{50} values in μM are indicated. Bepridil is effective against all native virus strains evaluated. Results are from two or more replicates. Error bars represent SE. The cytotoxicity of bepridil is shown by inhibiting Vero E6 proliferation without virus exposure.

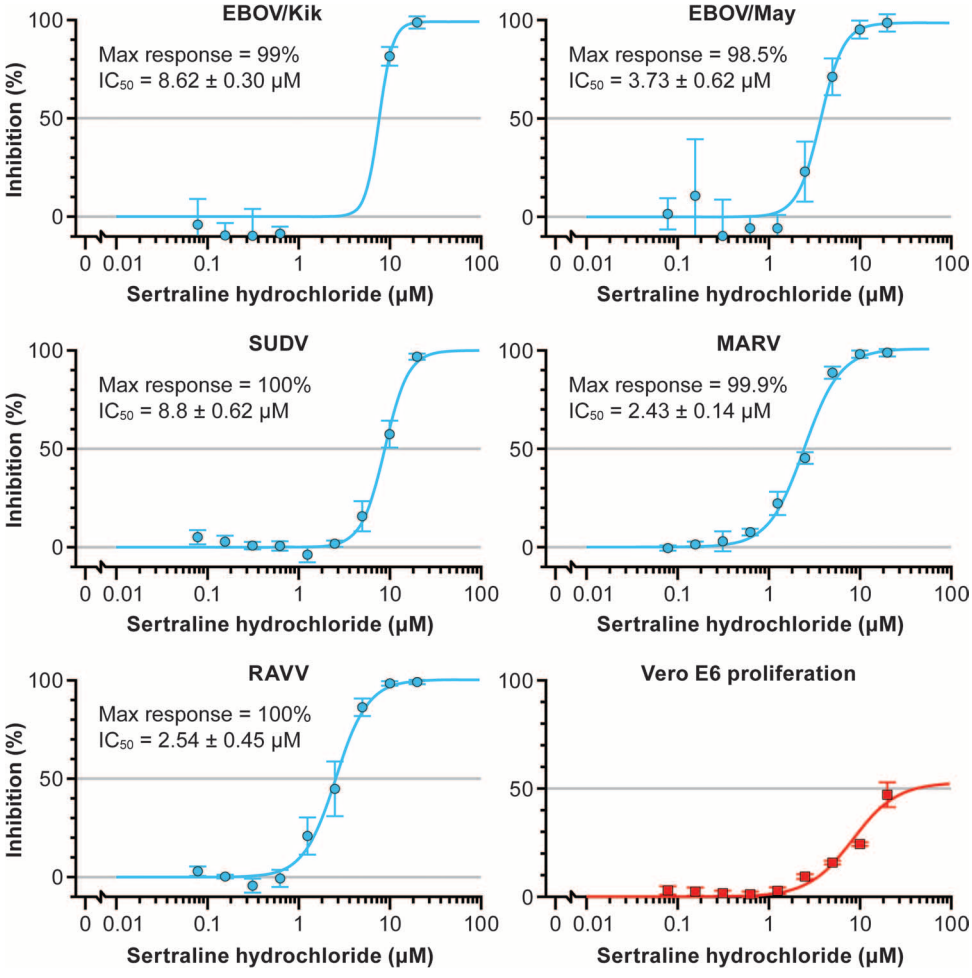

Fig. 8. In vitro dose-response curves for sertraline against native filovirus strains. The percent inhibition of bepridil against native filovirus strains [that is, EBOV/Kik (EBOV-95), EBOV/May (EBOV-76), SUDV, MARV, and RAVV] was evaluated by cell-based ELISA. The maximum percent inhibition (Max % response) of these strains and IC_{50} values in μM are indicated. Sertraline is effective across all native virus strains evaluated. Results are from two or more replicates. Error bars represent SE. The cytotoxicity of sertraline is shown by inhibiting Vero E6 proliferation without virus exposure.

is a long-acting nonselective calcium channel blocker targeting both L- and T-type calcium channels (*45*, *46*). Recently, the FDA-approved calcium channel blockers amiodarone, dronedarone, and verapamil were found to inhibit filovirus entry (*43*). Amiodarone (also a FIASMA) has a similar nonselective calcium channel profile as bepridil. Sakurai and colleagues determined that the endosomal two-pore calcium channel is important for mediating calcium signaling and subsequently EBOV cell entry (*44*). In addition to bepridil, we identified several calcium channel blockers including lomerizine, which can also antagonize L-type calcium channels (*47*).

We and others have investigated the utility of screening with approved drugs to identify potential therapeutics that can be used against EBOV and other biological threat agents or emerging diseases (*43*, *48*–*50*). Often with such diseases, conventional drug development is challenging because of both cost and ability to perform controlled clinical studies. Although new anti-EBOV therapeutics in the clinical pipeline show promise (*4*), it will be some time before these therapeutics are used in a routine clinical care setting. Use of new therapeutics may not be feasible in resource-constrained countries. By repurposing approved drugs, in theory, one may reduce the risk, time, and cost associated with therapeutic candidates. Researchers leverage already well-established safety and pharmacokinetic profiles and previous manufacturing and formulation experience of these approved drugs (*8*, *9*). Many drugs identified in our screen, such as bepridil and sertraline, are orally available and have established profiles of clinical use.

However, one of the great challenges of drug repurposing for an antiviral indication is achieving high enough human exposure to observe a clinical effect. Most of the drugs identified in our screen have in vitro IC_{50} values at fairly high micromolar concentrations. The human exposure of many drugs will only reach high nanomolar concentrations at peak serum concentrations (C_{max}). Thus, many of the drugs we identified in this screen may not be viable repurposing candidates for EBOV, because plasma concentrations where efficacy would be expected to be observed are not achievable. Higher doses of these drugs may be safe for use for a shorter duration of viral infection, especially for drugs approved for use chronically, and additional exploration of such doses may be required. Another consideration is repurposing these approved drugs in combination either with other approved drugs (identified in this and other screens) or with compounds in current EBOV clinical pipelines, which may improve therapeutic selectivity and present a higher bar to development of resistance (*13*).

We advanced bepridil and sertraline, in part, because both of these compounds have achievable human exposures with currently approved doses that are near IC_{50} values we observed in vitro in our eight-point dose-response screens. Bepridil has a human C_{max} of 3.72 μM at steady state (*51*). Bepridil has some cardiovascular side effects such as ventricular arrhythmia. The risk-to-benefit quotient of short-term use of bepridil to treat or prevent EBOV infection (with careful monitoring) will need to be considered. Sertraline has a long clinical history of use with approval for pediatrics diagnosed with obsessive-compulsive disorder. Although human sertraline exposure (C_{max} ~352 nM) may be much lower than the in vitro IC_{50}s we observed (*52*), it can concentrate in some organs (liver) targeted by EBOV by as much as 20-fold, and, therefore, appropriate concentrations may be obtained in some tissues targeted by EBOV (*53*). Sertraline is available off the shelf for distribution to patients, healthcare workers, and the greater community and may be of particular use as a prophylactic agent. Although both bepridil and sertraline showed significant survival benefits in a murine EBOV infection model, additional studies are required in a nonhuman primate EBOV model. Such a

model more closely mimics the human disease state than the murine model and can be used to further explore utility of these drugs as prophylactics and therapeutics against EBOV infection.

Screening of approved drugs is one avenue to identify potential treatments for viral threats such as EBOV. We will continue to evaluate bepridil, sertraline, and other drugs identified in our screen as therapeutics for EBOV either alone or in combination with other identified inhibitors.

MATERIALS AND METHODS

Study design

The purpose of this compound screen was to test a pharmacopeia library for anti-EBOV activity in an agnostic fashion to identify novel inhibitors. All compounds in the library were plated and tested in vitro for antiviral activity, with the identities of the compound and screening order blinded to the experimenters and the testing laboratory. For all studies using live virus, a minimum of two replicates were performed on separate days. For entry studies, two to three replicates were performed on the same day for each experiment.

For in vivo studies, sample sizes were selected to minimize the number of animals needed to obtain a statistically significant result. Animals were randomly assigned to study arms. Animal studies were not blinded to the study investigators but were blinded to personnel performing treatment injections. Cage weights were used to determine an average mouse weight for treatment purposes.

Ethics statement

Animal research was conducted under a protocol approved by Institutional Animal Care and Use Committee at U.S. Army Medical Research Institute of Infectious Diseases (USAMRIID) (U.S. Department of Agriculture registration number 51-F-0021/728 and Office of Laboratory Animal Welfare assurance number A3473-01) in compliance with the Animal Welfare Act and other federal statutes and regulations relating to animals and experiments involving animals. The facility where this research was conducted is fully accredited by the Association for Assessment and Accreditation of Laboratory Animal Care, International and adheres to principles stated in the *Guide for the Care and Use of Laboratory Animals* (National Research Council, 2011).

Live virus experiments

Experiments using live filoviruses were performed in biosafety level 4 (BSL-4) facilities at USAMRIID. Personnel wore positive-pressure protective suits fitted with high-efficiency particulate air filters and umbilical-fed air. USAMRIID is registered with the U.S. Centers for Disease Control and Prevention (CDC) Select Agent Program for the possession and use of biological select agents and toxins and has implemented a biological surety program in accordance with U.S. Army Regulation AR 50-1 "Biological Surety."

Reagents

Astemizole [chemical abstracts service (CAS) #68844-77-9], fluphenazine hydrochloride (CAS #146-56-5), hycanthone (CAS #3105-97-3), pimozide (CAS #2062-78-4), prochlorperazine edisylate (CAS #1257-78-9), quinacrine dihydrochloride (CAS #69-05-6), terconazole (CAS #67915-31-5), and thioridazine (CAS #130-61-0) were purchased from MicroSource Discovery Systems. Ammonium chloride (CAS #12125-02-9), benztropine mesylate (CAS #132-17-2), bepridil hydrochloride monohydrate (CAS #74764-40-2), clomiphene citrate (CAS #50-41-9), clomipramine hydrochloride (CAS #17321-77-6), flupentixol dihydrochloride (CAS #51529-01-2), EIPA (CAS #1154-25-2), maprotiline hydrochloride (CAS #10347-81-6), strophanthin (CAS #11005-63-3), and vinorelbine tartrate hydrate (CAS #125317-39-7) were purchased from Sigma-Aldrich. Aripiprazole (CAS #129722-12-9), efavirenz (CAS #154598-52-4), lomerizine dihydrochloride (CAS #101477-54-7), mycophenolate mofetil (CAS #128794-94-5), simvastatin (CAS #79902-63-9), teicoplanin (CAS #61036-62-2), and toremifene citrate (CAS #89778-27-8) were purchased from Sequoia Research Products. Atovaquone (CAS #95233-18-4), azacitidine (CAS #320-67-2), and clemastine fumarate (CAS #14976-57-9) were purchased from Selleck Chemicals. Dasatinib (CAS #302962-49-8) and sertraline hydrochloride (CAS #79559-97-0) were purchased from Toronto Research Chemicals. EST (E64d) was purchased from Cayman Chemical Co. Paroxetine hydrochloride hemihydrate (CAS #110429-35-1) was purchased from LKT Laboratories. Piperacetazine (CAS #3819-00-9) was purchased from U.S. Pharmacopeia. U18666A (CAS #63177-57-1) was purchased from Enzo Life Sciences. Dimethyl sulfoxide (DMSO) was used as solvent for the high-throughput screening assay described below. The 9G4 antibody (*54*, *55*) was developed by M. Hevey *et al.* (USAMRIID, Fort Detrick). The 13C6 antibody was developed by J. Wilson *et al.* (USAMRIID, Fort Detrick) (*56*). The 3C10 antibody was provided by J. Dye (USAMRIID, Fort Detrick). The 9E12 antibody was developed and provided by D. Negley (USAMRIID, Fort Detrick).

Cells and viruses

Vero E6 cells [American Type Culture Collection (ATCC): CRL-1586] and HepG2 cells (ATCC: HB-8065) were maintained in Eagle's minimum essential medium (Gibco Invitrogen) supplemented with 10% fetal bovine serum (FBS; Gibco Invitrogen). 293AD cells (Agilent Technologies, 240085) and SNB19 cells (from W. Maury) were maintained in Dulbecco's modified Eagle's medium (DMEM; Gibco Invitrogen) supplemented with 10% FBS (Hyclone), 1% antibiotic/antimycotic, 1% L-glutamine, and 1% sodium pyruvate (Gibco Invitrogen).

The filoviruses—Ebola virus isolates Kikwit (EBOV-95 or EBOV/Kik), Mayinga (EBOV-76 or EBOV/May), eGFP-EBOV, SUDV, MARV, and RAVV—were replicated as described by Johansen *et al.* (*11*).

Screening assay and library

A compound library of 2635 compounds (table S1) composed of approved drugs, mechanistic probes, and elite compounds such as dietary supplements, vitamins, minerals, and food additives was compiled and used for this screen (*7*, *13*). For the screen, compounds were added directly to 96-well compound plates using either a MiniTrak (PerkinElmer) or an acoustic compound dispenser (Echo 555, Labcyte). Compounds were suspended in a final volume of 200 μl of DMEM at 4× the final concentration, and plates were frozen at −80°C for a minimum of 24 hours and shipped to investigators at USAMRIID. Compound plates were thawed before the addition of compound to the infectivity assay described below. For the screens, compounds were plated in 200 μl of medium at 4× the final concentration, such that the addition of 50 μl to assay plates resulted in the appropriate final concentration (200 μl final assay volume after virus addition).

The screening assay for EBOV used a genetically engineered Ebola virus expressing eGFP, eGFP-EBOV (*12*), and the virus was provided by

J. Towner of the CDC. The screening assay was performed as described by Johansen *et al.* (*11*). Briefly, Vero E6 or HepG2 cells were plated in 96-well plates at a density of 40,000 cells per well in a total volume of 100 µl per well and incubated overnight at 37°C and 5% CO_2. Next, 50 µl of the prediluted compounds was added at a 4× concentration to each well to achieve the desired final concentration. Finally, 50 µl of the indicated virus or medium (corresponding to an approximate multiplicity of infection of 0.2) was added to cells. These assay plates were incubated for 48 hours at 37°C and 5% CO_2. After incubation, the amount of fluorescence in each well of the infected plates was determined using a spectrofluorometer (Molecular Devices; excitation: 485 nm, emission: 515 nm, cutoff: 495 nm). Antiviral activity was calculated by the inhibition of eGFP of treated cells compared to mock-treated control cells. The average signal for the eGFP assay was 1780 (±11) fluorescent light units (FLUs). The background was 61 (±2) FLUs. The signal/noise (S/N) ratio was 29 for the screen.

Compounds were tested at three concentrations in the preliminary screen against eGFP-EBOV infection and were considered active if the antiviral activity observed was >40% inhibition (*I*) with no or low corresponding cytotoxicity. The in vitro anti-EBOV activity of 30 compounds was confirmed by testing compounds at seven serially diluted doses in both Vero E6 and HepG2 cells.

To confirm that a decrease in fluorescence correlated with the inhibition of viral replication and not an increase in cell death, a counter screen was run in tandem using uninfected Vero E6 or HepG2 cells. Cells were seeded in 96-well plates as described above and incubated overnight at 37°C and 5% CO_2. The following day, cells were treated with compound and mock-infected with medium. After 48 hours of incubation, cell viability was assessed using the CellTiter-Glo Luminescent Cell Viability Assay Kit (Promega). This assay measures the concentrations of adenosine triphosphate (ATP) in the lysed cells in each well, with higher concentrations of ATP correlating with greater cellular viability. Thus, a compound with antiviral activity is expected to inhibit the emission fluorescence measured by relative luminescent light units (RLUs) with minimal effect on the ATP concentrations measured by the CellTiter-Glo assay. The average signal for the assay as measured by a SpectraMax M5 (Molecular Devices) was 305,300 (±1500) RLUs, with a background signal of 1580 (±40) RLUs for an S/N ratio of 193.

EBOV entry and internalization assays

The BlaM entry assay (*57*) was adapted for assessing effects of candidate inhibitory compounds on EBOV-VLP entry as described in (*11*, *14*). Briefly, 293AD cells were pretreated for 60 min with the indicated concentration of the active compound or with DMSO vehicle in Opti-MEM medium (Life Technologies). Cells were cooled on ice and VLPs were added and concentrated at the cell surface by spinfection, after which cells were incubated at 37°C for 3 hours. Cells were washed with loading medium, and CCF2/AM dye, a BlaM substrate that fluoresces blue when cleaved, was added. Cells were incubated overnight in loading medium, fixed, and analyzed by flow cytometry with a FACSCalibur flow cytometer (BD Biosciences). The percentage of cells showing VLP entry was calculated as the ratio of the number of blue cells to the total number of cells gated. VLP internalization was assessed using the same stock of VLPs, but assessment relied on their content of mCherry-VP40 instead of BlaM-VP40 (*14*). All flow cytometric data for both the VLP internalization and entry assays were analyzed using the FlowJo software package.

Murine Ebola virus infection model

The murine Ebola virus infection model was as described previously (*17*, *18*). ma-EBOV was obtained from M. Bray (Virology Division, USAMRIID). C57BL/6 mice (5 to 8 weeks old) were obtained from the National Cancer Institute and housed under specific pathogen–free conditions. C57BL/6 mice were injected intraperitoneally with a target dose of 1000 PFU of the ma-EBOV in a BSL-4 laboratory at USAMRIID. A stock (50 mg/ml) of each compound was generated in 100% DMSO and diluted with phosphate-buffered saline (PBS) to obtain the final treatment concentration. Animals were treated BID starting 1 hour after challenge with either sertraline (10 mg/kg in 0.225% DMSO/PBS) or bepridil (12 mg/kg in 2.4% DMSO/PBS). In other studies, mice were treated with clomipramine (45 mg/kg in 9% DMSO/PBS) once daily (QD), lomerizine (22 mg/kg in 4.4% DMSO/PBS) QD, aripiprazole (20 mg/kg in 0.225% DMSO/PBS) BID, teicoplanin (14 mg/kg in 2.8% DMSO/PBS) QD, paroxetine (15 mg/kg in 3% DMSO/PBS) QD, and efavirenz (15 mg/kg in 3% DMSO/PBS) BID 1 hour after challenge. Compounds were administered to mice by intraperitoneal injection with a total injection volume of 200 µl. Mice in the vehicle control groups were administered a solution of 5% DMSO/PBS without drug. Animals were treated for a total of 10 days and monitored for survival for a total of 28 days after virus exposure.

VLP preparation

For the VLP entry and internalization assays, VLPs were prepared as described in (*11*, *14*). VLPs expressing VSV-G or LCMV-GP were prepared as described by Johansen *et al.* (*11*).

Cathepsin activity and endosome acidification assays

Cathepsin B activity in cell lysates adjusted to pH of 5 was assayed using the cathepsin B substrate *N*-benzyloxycarbonyl-L-arginyl-L-arginine-7-amido-4-methylcoumarin (Calbiochem), as described in (*58*). Cathepsin L was assayed the same as cathepsin B, but using the cathepsin L substrate *N*-benzyloxycarbonyl-L-phenylalanyl-L-arginine-7-amido-4-methylcoumarin (Calbiochem) in the presence of 1 µM CA074, a cathepsin B inhibitor (Calbiochem). Combined activity of cathepsins B plus L was assayed as above using the cathepsin L substrate in the absence of any inhibitor. Endosomal acidification was analyzed as described by Johansen *et al.* (*11*).

In vitro EBOV trafficking assays

Colocalization between EBOV-VLP–$GP_{1,2}$ and $NPC1^+$ endolysosomes was determined as described by Mingo *et al.* (*30*), with the following minor modifications: 293AD cells were seeded into eight-well chamber slides (75,000 cells per well). After about 16 hours, the cells were pretreated with vehicle (DMSO, mock) or the indicated concentration of the active compound for 1 hour at 37°C. The cells were then chilled to 15°C for 30 min, VLPs tagged with mCherry-VP40 (± drugs) were added, and the cells were incubated for an additional 60 min (at 15°C) to allow VLP binding and internalization. The cells were then warmed to 37°C for 100 min, fixed, stained for NPC1, imaged, and analyzed as described by Mingo *et al.* (*30*).

Pseudovirion infection

VSV pseudovirions bearing Ebola virus GP (VSV-GP) and encoding GFP were produced as described previously (*15*). Infection of the parental CHO or NPC1-overexpressing CHO cells was performed as described in (*14*).

Native filovirus strain ELISA

Cell-based ELISA assays using native strains of virus, EBOV/Kik, EBOV/May, SUDV, MARV, or RAVV have been previously described by Johansen *et al.* (*11*). The signal for the EBOV/Kik assay was 137,400 (±4100) RLUs with an S/N ratio of 159. The signal for the EBOV/May assay was 45,600 (±2600) RLUs with an S/N ratio of 95. The signal for the SUDV assay was 188,400 (±2750) RLUs with an S/N ratio of 74. The signal for the MARV assay was 55,000 (±1400) RLUs with an S/N ratio of 102. The signal for the RAVV assay was 175,000 (±10,000) RLUs with an S/N ratio of 124.

Data analysis

For the eGFP-EBOV screen and native strain ELISA assays, raw phenotype measurements T from each treated well were converted to normalized fractional inhibition $I = 1 - T/V$ relative to the median of vehicle-treated V wells arranged around the plate. After normalization, average activity values were calculated between replicate measurements at the same treatment doses along with σ_1, the accompanying SE estimates. Drug response curves were represented by a logistic sigmoidal function with a maximal effect level (A_{max}), the concentration at half-maximal activity of the compound (EC_{50}), and a Hill coefficient representing the sigmoidal transition. All curve fits were through the zero-concentration point. We used the fitted curve parameters to calculate the concentration (IC_{50}) at which the drug response reached an absolute inhibition of 50%, limited to the maximum tested concentration for inactive compounds.

Statistical analysis

For mice studies evaluating the efficacy of sertraline, bepridil, and compounds listed in table S3, the mean time to death was analyzed by analysis of variance (ANOVA) comparing only those mice that succumbed before the study ended. Because of the sample size used for these studies, differences in overall survival between treatment and vehicle control groups were evaluated using Fisher's exact test (with step-down Bonferroni adjustment where necessary). A *P value* of <0.05 indicates a significant difference between experimental groups. Time to death was compared to control using only animals that succumbed. For studies investigating the mechanism by which bepridil and sertraline block VLP entry into the cytoplasm, values for drug-treated samples were compared to those for mock-treated samples using Student's *t* tests (two-tailed assuming equal variances). A *P value* of <0.001 indicates a significant difference between experimental groups. All statistics conform to the journal's policy.

SUPPLEMENTARY MATERIALS

www.sciencetranslationalmedicine.org/cgi/content/full/7/290/290ra89/DC1

Table S1. Results of a three-point dose antiviral screen of 2635 compounds against eGFP-EBOV infection (two Excel files).

Table S2. Active compounds identified from preliminary three-point dose antiviral screen against eGFP-EBOV infection (Excel file).

Table S3. Survival of ma-EBOV–infected C57BL/6 mice after treatment with additional priority active compounds identified in vitro.

Fig. S1. Comparison of compound activity in the antiviral assay against eGFP-EBOV infection versus uninfected host cell proliferation.

Fig. S2. Confirmatory in vitro eight-point dose-response curves for active compounds from EBOV antiviral screen in Vero E6 cells.

Fig. S3. Additional confirmatory in vitro eight-point dose-response curves for active compounds from EBOV antiviral screen in Vero E6 cells.

Fig. S4. Confirmatory in vitro eight-point dose-response curves for active compounds from EBOV antiviral screen in HepG2 cells.

Fig. S5. Additional confirmatory in vitro eight-point dose-response curves for active compounds from EBOV antiviral screen in HepG2 cells.

Fig. S6. Evaluation of sertraline and bepridil on endosome acidification.

Fig. S7. Evaluation of sertraline and bepridil on EBOV-VLP–$GP_{1,2}$ trafficking to $NPC1^+$ endolysosomes.

Fig. S8. Bepridil and sertraline, at the indicated concentrations, do not inhibit the viability of 293AD cells.

Fig. S9. Assessment of bepridil and sertraline on VSV EBOV-GP pseudovirion entry into parental and NPC1-overexpressing CHO cell lines.

REFERENCES AND NOTES

1. S. Mahanty, M. Bray, Pathogenesis of filoviral haemorrhagic fevers. *Lancet Infect. Dis.* **4**, 487–498 (2004).
2. T. W. Geisbert, A. C. Lee, M. Robbins, J. B. Geisbert, A. N. Honko, V. Sood, J. C. Johnson, S. de Jong, I. Tavakoli, A. Judge, L. E. Hensley, I. Maclachlan, Postexposure protection of non-human primates against a lethal Ebola virus challenge with RNA interference: A proof-of-concept study. *Lancet* **375**, 1896–1905 (2010).
3. World Health Organization, Ebola virus disease; http://www.who.int/mediacentre/factsheets/fs103/en/.
4. T. W. Geisbert, L. E. Hensley, Ebola virus: New insights into disease aetiopathology and possible therapeutic interventions. *Expert Rev. Mol. Med.* **6**, 1–24 (2004).
5. M. Chan, WHO Director-General addresses the UN Economic and Social Council on the Ebola threat. Keynote address at the Special Meeting of the Economic and Social Council on "Ebola: A threat to economic and social progress," New York, NY, 5 December 2014; http://www.who.int/dg/speeches/2014/ecosoc-ebola-meeting/en/.
6. G. Wong, X. Qiu, G. G. Olinger, G. P. Kobinger, Post-exposure therapy of filovirus infections. *Trends Microbiol.* **22**, 456–463 (2014).
7. A. A. Borisy, P. J. Elliott, N. W. Hurst, M. S. Lee, J. Lehár, E. R. Price, G. Serbedzija, G. R. Zimmermann, M. A. Foley, B. R. Stockwell, C. T. Keith, Systematic discovery of multicomponent therapeutics. *Proc. Natl. Acad. Sci. U.S.A.* **100**, 7977–7982 (2003).
8. T. T. Ashburn, K. B. Thor, Drug repositioning: Identifying and developing new uses for existing drugs. *Nat. Rev. Drug Discov.* **3**, 673–683 (2004).
9. C. R. Chong, D. J. Sullivan Jr., New uses for old drugs. *Nature* **448**, 645–646 (2007).
10. M. Garcia, A. Cooper, W. Shi, W. Bornmann, R. Carrion, D. Kalman, G. J. Nabel, Productive replication of Ebola virus is regulated by the c-Abl1 tyrosine kinase. *Sci. Transl. Med.* **4**, 123ra124 (2012).
11. L. M. Johansen, J. M. Brannan, S. E. Delos, C. J. Shoemaker, A. Stossel, C. Lear, B. G. Hoffstrom, L. E. DeWald, K. L. Schornberg, C. Scully, J. Lehár, L. E. Hensley, J. M. White, G. G. Olinger, FDA-approved selective estrogen receptor modulators inhibit Ebola virus infection. *Sci. Transl. Med.* **5**, 190ra179 (2013).
12. J. S. Towner, J. Paragas, J. E. Dover, M. Gupta, C. S. Goldsmith, J. W. Huggins, S. T. Nichol, Generation of eGFP expressing recombinant Zaire ebolavirus for analysis of early pathogenesis events and high-throughput antiviral drug screening. *Virology* **332**, 20–27 (2005).
13. J. Lehár, A. S. Krueger, W. Avery, A. M. Heilbut, L. M. Johansen, E. R. Price, R. J. Rickles, G. F. Short, III, J. E. Staunton, X. Jin, M. S. Lee, G. R. Zimmermann, A. A. Borisy, Synergistic drug combinations tend to improve therapeutically relevant selectivity. *Nat. Biotechnol.* **27**, 659–666 (2009).
14. C. J. Shoemaker, K. L. Schornberg, S. E. Delos, C. Scully, H. Pajouhesh, G. G. Olinger, L. M. Johansen, J. M. White, Multiple cationic amphiphiles induce a niemann-pick C phenotype and inhibit Ebola virus entry and infection. *PLOS One* **8**, e56265 (2013).
15. K. Schornberg, S. Matsuyama, K. Kabsch, S. Delos, A. Bouton, J. White, Role of endosomal cathepsins in entry mediated by the Ebola virus glycoprotein. *J. Virol.* **80**, 4174–4178 (2006).
16. D. Dube, K. L. Schornberg, C. J. Shoemaker, S. E. Delos, T. S. Stantchev, K. A. Clouse, C. C. Broder, J. M. White, Cell adhesion-dependent membrane trafficking of a binding partner for the ebolavirus glycoprotein is a determinant of viral entry. *Proc. Natl. Acad. Sci. U.S.A.* **107**, 16637–16642 (2010).
17. M. Bray, K. Davis, T. Geisbert, C. Schmaljohn, J. Huggins, A mouse model for evaluation of prophylaxis and therapy of Ebola hemorrhagic fever. *J. Infect. Dis.* **178**, 651–661 (1998).
18. M. Bray, K. Davis, T. Geisbert, C. Schmaljohn, J. Huggins, A mouse model for evaluation of prophylaxis and therapy of Ebola hemorrhagic fever. *J. Infect. Dis.* **179**, S248–S258 (1999).
19. C. L. Hunt, N. J. Lennemann, W. Maury, Filovirus entry: A novelty in the viral fusion world. *Viruses* **4**, 258–275 (2012).
20. J. M. White, K. L. Schornberg, A new player in the puzzle of filovirus entry. *Nat. Rev. Microbiol.* **10**, 317–322 (2012).
21. A. Nanbo, M. Imai, S. Watanabe, T. Noda, K. Takahashi, G. Neumann, P. Halfmann, Y. Kawaoka, Ebolavirus is internalized into host cells via macropinocytosis in a viral glycoprotein-dependent manner. *PLOS Pathog.* **6**, e1001121 (2010).

22. M. A. Brindley, L. Hughes, A. Ruiz, P. B. McCray Jr., A. Sanchez, D. A. Sanders, W. Maury, Ebola virus glycoprotein 1: Identification of residues important for binding and postbinding events. *J. Virol.* **81**, 7702–7709 (2007).
23. K. Chandran, N. J. Sullivan, U. Felbor, S. P. Whelan, J. M. Cunningham, Endosomal proteolysis of the Ebola virus glycoprotein is necessary for infection. *Science* **308**, 1643–1645 (2005).
24. J. E. Carette, M. Raaben, A. C. Wong, A. S. Herbert, G. Obernosterer, N. Mulherkar, A. I. Kuehne, P. J. Kranzusch, A. M. Griffin, G. Ruthel, P. Dal Cin, J. M. Dye, S. P. Whelan, K. Chandran, T. R. Brummelkamp, Ebola virus entry requires the cholesterol transporter Niemann–Pick C1. *Nature* **477**, 340–343 (2011).
25. M. Côté, J. Misasi, T. Ren, A. Bruchez, K. Lee, C. M. Filone, L. Hensley, Q. Li, D. Ory, K. Chandran, J. Cunningham, Small molecule inhibitors reveal Niemann–Pick C1 is essential for Ebola virus infection. *Nature* **477**, 344–348 (2011).
26. E. H. Miller, G. Obernosterer, M. Raaben, A. S. Herbert, M. S. Deffieu, A. Krishnan, E. Ndungo, R. G. Sandesara, J. E. Carette, A. I. Kuehne, G. Ruthel, S. R. Pfeffer, J. M. Dye, S. P. Whelan, T. R. Brummelkamp, K. Chandran, Ebola virus entry requires the host-programmed recognition of an intracellular receptor. *EMBO J.* **31**, 1947–1960 (2012).
27. M. Brecher, K. L. Schornberg, S. E. Delos, M. L. Fusco, E. O. Saphire, J. M. White, Cathepsin cleavage potentiates the Ebola virus glycoprotein to undergo a subsequent fusion-relevant conformational change. *J. Virol.* **86**, 364–372 (2012).
28. D. Dube, M. B. Brecher, S. E. Delos, S. C. Rose, E. W. Park, K. L. Schornberg, J. H. Kuhn, J. M. White, The primed ebolavirus glycoprotein (19-kilodalton $GP_{1,2}$): Sequence and residues critical for host cell binding. *J. Virol.* **83**, 2883–2891 (2009).
29. S. Bale, T. Liu, S. Li, Y. Wang, D. Abelson, M. Fusco, V. L. Woods Jr., E. O. Saphire, Ebola virus glycoprotein needs an additional trigger, beyond proteolytic priming for membrane fusion. *PLOS Negl. Trop. Dis.* **5**, e1395 (2011).
30. R. M. Mingo, J. A. Simmons, C. J. Shoemaker, E. A. Nelson, K. L. Schornberg, R. S. D'Souza, J. E. Casanova, J. M. White, Ebola virus and severe acute respiratory syndrome coronavirus display late cell entry kinetics: Evidence that transport to $NPC1^+$ endolysosomes is a rate-defining step. *J. Virol.* **89**, 2931–2943 (2015).
31. W. Knecht, J. Henseling, M. Löffler, Kinetics of inhibition of human and rat dihydroorotate dehydrogenase by atovaquone, lawsone derivatives, brequinar sodium and polyporic acid. *Chem. Biol. Interact.* **124**, 61–76 (2000).
32. G. Leone, M. T. Voso, L. Teofili, M. Lübbert, Inhibitors of DNA methylation in the treatment of hematological malignancies and MDS. *Clin. Immunol.* **109**, 89–102 (2003).
33. M. J. Dapp, C. L. Clouser, S. Patterson, L. M. Mansky, 5-Azacytidine can induce lethal mutagenesis in human immunodeficiency virus type 1. *J. Virol.* **83**, 11950–11958 (2009).
34. M. Khan, R. Dhanwani, I. K. Patro, P. V. Rao, M. M. Parida, Cellular IMPDH enzyme activity is a potential target for the inhibition of Chikungunya virus replication and virus induced apoptosis in cultured mammalian cells. *Antiviral Res.* **89**, 1–8 (2011).
35. R. Takhampunya, S. Ubol, H.-S. Houng, C. E. Cameron, R. Padmanabhan, Inhibition of dengue virus replication by mycophenolic acid and ribavirin. *J. Gen. Virol.* **87**, 1947–1952 (2006).
36. F. A. Carvalho, F. A. Carneiro, I. C. Martins, I. Assunção-Miranda, A. F. Faustino, R. M. Pereira, P. T. Bozza, M. A. Castanho, R. Mohana-Borges, A. T. Da Poian, N. C. Santos, Dengue virus capsid protein binding to hepatic lipid droplets (LD) is potassium ion dependent and is mediated by LD surface proteins. *J. Virol.* **86**, 2096–2108 (2012).
37. A. Kapoor, H. Cai, M. Forman, R. He, M. Shamay, R. Arav-Boger, Human cytomegalovirus inhibition by cardiac glycosides: Evidence for involvement of the HERG gene. *Antimicrob. Agents Chemother.* **56**, 4891–4899 (2012).
38. A. K. Karuppannan, K. X. Wu, J. Qiang, J. J. Chu, J. Kwang, Natural compounds inhibiting the replication of Porcine reproductive and respiratory syndrome virus. *Antiviral Res.* **94**, 188–194 (2012).
39. J. Kornhuber, P. Tripal, M. Reichel, C. Muhle, C. Rhein, M. Muehlbacher, T. W. Groemer, E. Gulbins, Functional inhibitors of acid sphingomyelinase (FIASMAs): A novel pharmacological group of drugs with broad clinical applications. *Cell. Physiol. Biochem.* **26**, 9–20 (2010).
40. J. Kornhuber, M. Muehlbacher, S. Trapp, S. Pechmann, A. Friedl, M. Reichel, C. Mühle, L. Terfloth, T. W. Groemer, G. M. Spitzer, K. R. Liedl, E. Gulbins, P. Tripal, Identification of novel functional inhibitors of acid sphingomyelinase. *PLOS One* **6**, e23852 (2011).
41. M. E. Miller, S. Adhikary, A. A. Kolokoltsov, R. A. Davey, Ebolavirus requires acid sphingomyelinase activity and plasma membrane sphingomyelin for infection. *J. Virol.* **86**, 7473–7483 (2012).
42. A. G. Lee, Effects of charged drugs on the phase transition temperatures of phospholipid bilayers. *Biochim. Biophys. Acta* **514**, 95–104 (1978).
43. G. Gehring, K. Rohrmann, N. Atenchong, E. Mittler, S. Becker, F. Dahlmann, S. Pöhlmann, F. W. Vondran, S. David, M. P. Manns, S. Ciesek, T. von Hahn, The clinically approved drugs amiodarone, dronedarone and verapamil inhibit filovirus cell entry. *J. Antimicrob. Chemother.* **69**, 2123–2131 (2014).
44. Y. Sakurai, A. A. Kolokoltsov, C. C. Chen, M. W. Tidwell, W. E. Bauta, N. Klugbauer, C. Grimm, C. Wahl-Schott, M. Biel, R. A. Davey, Two-pore channels control Ebola virus host cell entry and are drug targets for disease treatment. *Science* **347**, 995–998 (2015).
45. C. J. Cohen, S. Spires, D. Van Skiver, Block of T-type Ca channels in guinea pig atrial cells by antiarrhythmic agents and Ca channel antagonists. *J. Gen. Physiol.* **100**, 703–728 (1992).
46. I. Kodama, K. Kamiya, J. Toyama, Cellular electropharmacology of amiodarone. *Cardiovasc. Res.* **35**, 13–29 (1997).
47. L. T. Tran, B. J. Gentil, K. E. Sullivan, H. D. Durham, The voltage-gated calcium channel blocker lomerizine is neuroprotective in motor neurons expressing mutant SOD1, but not TDP-43. *J. Neurochem.* **130**, 455–466 (2014).
48. J. Dyall, C. M. Coleman, B. J. Hart, T. Venkataraman, M. R. Holbrook, J. Kindrachuk, R. F. Johnson, G. G. Olinger Jr., P. B. Jahrling, M. Laidlaw, L. M. Johansen, C. M. Lear-Rooney, P. J. Glass, L. E. Hensley, M. B. Frieman, Repurposing of clinically developed drugs for treatment of Middle East respiratory syndrome coronavirus infection. *Antimicrob. Agents Chemother.* **58**, 4885–4893 (2014).
49. P. B. Madrid, S. Chopra, I. D. Manger, L. Gilfillan, T. R. Keepers, A. C. Shurtleff, C. E. Green, L. V. Iyer, H. H. Dilks, R. A. Davey, A. A. Kolokoltsov, R. Carrion Jr., J. L. Patterson, S. Bavari, R. G. Panchal, T. K. Warren, J. B. Wells, W. H. Moos, R. L. Burke, M. J. Tanga, A systematic screen of FDA-approved drugs for inhibitors of biological threat agents. *PLOS One* **8**, e60579 (2013).
50. Z. L. Newman, N. Sirianni, C. Mawhinney, M. S. Lee, S. H. Leppla, M. Moayeri, L. M. Johansen, Auranofin protects against anthrax lethal toxin-induced activation of the Nlrp1b inflammasome. *Antimicrob. Agents Chemother.* **55**, 1028–1035 (2011).
51. L. M. Hollingshead, D. Faulds, A. Fitton, Bepridil. A review of its pharmacological properties and therapeutic use in stable angina pectoris. *Drugs* **44**, 835–857 (1992).
52. M. Reis, A. Åberg-Wistedt, H. Ågren, P. Höglund, A.-C. Åkerblad, F. Bengtsson, Serum disposition of sertraline, N-desmethylsertraline and paroxetine: A pharmacokinetic evaluation of repeated drug concentration measurements during 6 months of treatment for major depression. *Hum. Psychopharmacol.* **19**, 283–291 (2004).
53. B. Levine, A. J. Jenkins, J. E. Smialek, Distribution of sertraline in postmortem cases. *J. Anal. Toxicol.* **18**, 272–274 (1994).
54. M. Hevey, D. Negley, J. Geisbert, P. Jahrling, A. Schmaljohn, Antigenicity and vaccine potential of Marburg virus glycoprotein expressed by baculovirus recombinants. *Virology* **239**, 206–216 (1997).
55. M. Hevey, D. Negley, A. Schmaljohn, Characterization of monoclonal antibodies to Marburg virus (strain Musoke) glycoprotein and identification of two protective epitopes. *Virology* **314**, 350–357 (2003).
56. J. A. Wilson, M. Hevey, R. Bakken, S. Guest, M. Bray, A. L. Schmaljohn, M. K. Hart, Epitopes involved in antibody-mediated protection from Ebola virus. *Science* **287**, 1664–1666 (2000).
57. M. Cavrois, C. De Noronha, W. C. Greene, A sensitive and specific enzyme-based assay detecting HIV-1 virion fusion in primary T lymphocytes. *Nat. Biotechnol.* **20**, 1151–1154 (2002).
58. D. H. Ebert, J. Deussing, C. Peters, T. S. Dermody, Cathepsin L and cathepsin B mediate reovirus disassembly in murine fibroblast cells. *J. Biol. Chem.* **277**, 24609–24617 (2002).

Acknowledgments: Zalicus Inc. is now Epirus Biopharmaceuticals. The drug screening platform used for the work described here is now a division of Horizon Discovery Inc. We thank J. Towner (CDC) for the eGFP-expressing Ebola virus Zaire; M. Bray (USAMRIID) for providing ma-EBOV used in the animal studies; J. Dye (USAMRIID) for providing the monoclonal antibody used in our Ebola virus Sudan screen; D. Negley (USAMRIID) for the antibody used in the RAVV screen; and W. Maury (Department of Microbiology, Carver College of Medicine, University of Iowa) for the SNB19 cells. We thank J. Pettitt, K. DeRoche, C. Markwood, D. Julias, H. Esham, and S. Stronsky for technical assistance. We thank L. Bollinger (Integrated Research Facility, Fort Detrick) for technical writing services and J. Wada (Integrated Research Facility, Fort Detrick) for preparing figures for this paper. **Funding:** This work is funded by Defense Threat Reduction Agency project 4.10007_08_RD_B awarded to G.G.O. and subcontract (W81XWH-08-0051) awarded to L.M.J. from USAMRIID and an NIH grant U54 AI057168 and DTRA subcontract W81XWH-12-P-0007 awarded to J. M.W. This research was performed while L.E.D. held a National Research Council Research Associateship Award at USAMRIID. Opinions, interpretations, conclusions, and recommendations are those of the authors and are not necessarily endorsed by the U.S. Army. **Author contributions:** L.M.J., B.G.H., J.L., P.J.G., L.E.H., J.M.W., and G.G.O. designed the research; L.E.D., C.J.S., B.G.H., C.M.L.-R., A.S., E.N., S.E.D., J.A.S., J.M.G., and L.T.P. performed research; L.M.J., B.G.H., C.J.S., J.M.G., L.T.P., H.P., J.L., J.M.W., and G.G.O. analyzed data; and L.M.J., J.M.W., and G.G.O. wrote the paper. **Competing interests:** L.M.J., L.T.P., J.M.G., B.G.H., J. L., and H.P. were employed at Zalicus Inc. during the time the research was performed. J.M.G. is a shareholder at Horizon Discovery Inc. L.M.J. and G.G.O. holds a patent entitled "Composition and methods for the treatment of filovirus-mediated diseases," application no. 12710203. All other authors declare that they have no competing interests.

Submitted 23 December 2014
Accepted 13 May 2015
Published 3 June 2015
10.1126/scitranslmed.aaa5597

Citation: L. M. Johansen, L. E. DeWald, C. J. Shoemaker, B. G. Hoffstrom, C. M. Lear-Rooney, A. Stossel, E. Nelson, S. E. Delos, J. A. Simmons, J. M. Grenier, L. T. Pierce, H. Pajouhesh, J. Lehár, L. E. Hensley, P. J. Glass, J. M. White, G. G. Olinger, A screen of approved drugs and molecular probes identifies therapeutics with anti–Ebola virus activity. *Sci. Transl. Med.* **7**, 290ra89 (2015).